Notes

Semianalytical Continuum Model for Nondilute Neutral and Charged Brushes Including Finite Stretching

P. M. Biesheuvel,*,† W. M. de Vos,‡ and V. M. Amoskov§

Department of Environmental Technology, Wageningen University, Bomenweg 2, 6703 HD Wageningen, The Netherlands; Laboratory of Physical Chemistry and Colloid Science, Wageningen University, Dreijenplein 6, 6703 HB Wageningen, The Netherlands; and Institute of Macromolecular Compounds, Russian Academy of Sciences, Bol'shoi pr. 31, St. Petersburg, 199004 Russia

Received April 14, 2008
Revised Manuscript Received June 6, 2008

Introduction

The conformations of neutral and charged brushes is a topic of continuing interest, both experimentally[1,2] and theoretically.[3–5] In this Note we will analyze theories based on the strong-stretching limit of the self-consistent-field (SCF) equation (the polymer propagator equation). For relatively unstretched chains the Gaussian limit can be used which combined with the assumption of a dilute brush leads to the prediction of a parabolic density profile.[3,6–8] The end-density profile is relatively smooth and peaks relatively far from the edge of the brush: its position is ∼30% of the brush height away from the edge.

However, deviations from this dilute limit are well-analyzed theoretically using numerical and analytical theories for neutral brushes[4,9–15] and charged brushes.[16–18] Numerically, lattice-based implementations of the SCF equations, such as the Scheutjens−Fleer algoritm,[15,16,19] naturally include finite-stretching corrections as well as a description for volume exclusion that is also valid in the nondilute limit. Therefore, neither densities nor stretching degrees beyond unity are ever predicted, while the parabolic density profile only results in the dilute, unstretched, limit. Several analytical lattice-based SCF theories based on the strong stretching limit for neutral brushes include both corrections.[9,11,12,20] These expressions show how at high grafting density the density profile goes from a parabolic to a "block" profile, while the end-density profile becomes extremely peaked near the edge of the brush. The theories were applied to polyelectrolyte brushes,[20,21] brushes with concentration-dependent interactions,[13] and brushes immersed in a multicomponent solvent.[22]

These lattice-based analytical calculations are very useful as they show the essential physics of (strongly stretched) brushes. However, because they are based on the assumption of a lattice, there are also disadvantages. First of all, to observe in the theory the change from a parabola to a block profile in polymer density, and the sharp peak in end-segment distribution, very high grafting densities are required. This change in profile takes place between 60% and 80% of the anchoring sites containing a grafting monomer. Consequently, the polymer density is close to the maximum packing limit almost up to the edge of the brush. These are conditions that are not directly transferred to experimental parameter regimes. Indeed, it would be useful to have an *off-lattice* (semi)-analytical theory. In contrast to the lattice theories, in such an off-lattice theory grafting densities are dimensional (in number of anchoring points per unit surface area) and the Kuhn length (roughly speaking, a measure of chain stiffness) can be varied independently of the size of the monomers. In such a model we expect finite-stretching corrections to show up at much lower grafting densities than in the lattice approaches. Also, in the off-lattice approach we will discuss, it is relatively straightforward to implement the interaction of the brush with (mixtures of) ions and other entities (such as protein molecules) with sizes different from that of the polymer monomers.[23,24] This is a useful extension of the theory, which is not readily possible in lattice-based models.

However, a (semi)analytical SCF theory is not yet available for continuum chains (except in the Gaussian limit). Because theoretical investigations of nondilute brushes are becoming more important as advances in surface polymerization nowadays make the production and investigation of high-density brushes possible,[2] we develop in this Note a continuum SCF model valid for dense and strongly stretched brushes and show calculation results for polymer total density and end-density profiles, both for neutral and for charged brushes.

Theory

The strong-stretching limit of the SCF equation is based on assuming at each position in the brush [that is, at each position above the grafting interface; we take a mean-field approach in the lateral direction] the validity of the following equality[7,8]

$$V(h) - V(x) = \mu(\phi(x)) - \mu(\phi(h)) \tag{1}$$

where V is the "stretching" or SCF potential which is a function of distance from the interface, x, with h the brush height. Both x and h are dimensionless, scaled with the chain contour length [only monodisperse brushes are considered], $0 \le x \le h < 1$. For simple one-component solvents the constant $\mu(\phi(h))$ is usually chosen equal to zero, but in a more complex solvent this term cannot be omitted.[22] The mean-field interaction potential μ depends exclusively on the local interactions in the brush and does not depend on the conformational properties of the brush chains. It has many contributions including volume exclusion, enthalpic interactions, and electrostatics. In contrast, the SCF potential $V(x)$ does not depend on the local interaction inside the brush but characterizes the conformational properties of brush chains. It is different for the Gaussian model for chain stretching compared to models that include finite extensibility.[13]

For relatively unstretched brushes, the potential $V(x)$ is described by the Gaussian limit, which is given (per unit chain length) by[3,6–8]

* Corresponding author. E-mail: maarten.biesheuvel@wur.nl.
† Department of Environmental Technology, Wageningen University.
‡ Laboratory of Physical Chemistry and Colloid Science, Wageningen University.
§ Russian Academy of Sciences.

10.1021/ma800828c CCC: $40.75
Published on Web 07/30/2008

$$V(x) = \frac{3\pi^2}{8k} x^2 \tag{2}$$

where k is the Kuhn length.

Before discussing $\mu(\phi)$, let us first give the overall mass balance given by

$$\sigma\varepsilon = \int_0^h \phi \, dx \tag{3}$$

where σ is the grafting density (in numbers per unit area) and ε the brush volume per unit chain length. If we describe the brush as a flexible cylinder with diameter d, then $\varepsilon = \pi/4 \cdot d^2$, and if we model it as a string-of-touching spherical beads, $\varepsilon = \pi/6 \cdot d^2$ where d is the sphere diameter.

Now, in general we can describe $\mu(\phi)$ as an expansion

$$\mu(\phi) = v\phi + w\phi^2 + ... \tag{4}$$

where v is the second virial coefficient and w the third coefficient. Also in the case of charged brushes it is possible to describe μ as a polynomial function of the local density ϕ, but only as long as local electroneutrality can be assumed.

For completeness we give the solutions for polymer density profile $\phi(x)$ and end-density g(x) using for V the Gaussian result given by eq 2 and with μ given by eq 4, with terms beyond $w\phi^2$ omitted. We discuss (1) the case that $v \neq 0$ and $w = 0$ (dilute limit or athermal case) and (2) the case that $v = 0$ and $w \neq 0$ (polymer in a Θ-solvent).

For the athermal situation ($w = 0$), we obtain for brush height[6,13,15]

$$h = \sqrt[3]{\sigma\varepsilon \frac{8k}{3\pi^2} v} \tag{5}$$

and for $\phi(x)$ the well-known parabolic profile, given by[6,13–15]

$$\phi(x) = \frac{3\pi^2}{8vk}(h^2 - x^2) \tag{6}$$

The end-segment density distribution, $g(x)$, is given by[6,13–15]

$$g(x) = \frac{1}{\sigma\varepsilon} \frac{4\pi^2}{3vk} x\sqrt{h^2 - x^2} \tag{7}$$

which peaks at $x = 1/\sqrt{2}h \sim 0.71h$.

For the Θ-solvent ($v = 0$) and with only the third virial coefficient w assumed nonzero, the results are somewhat different; namely, the brush height is given by[15]

$$h = \sqrt{\frac{8\sigma\varepsilon}{\pi^2}\sqrt{\frac{2wk}{3}}} \tag{8}$$

while the polymer density profile follows an elliptical profile, given by[15]

$$\phi(x) = \sqrt{\frac{3\pi^2}{8wk}(h^2 - x^2)} \tag{9}$$

and the end-density distribution linearly increases with x (ref 15) and peaks at the edge of the brush, $g(x) = cx$, with the prefactor c given by $c = (\pi^2/4\sigma\varepsilon)[3/(2wk)]^{1/2}$.

Now, eqs 2 and 4 cannot be used for dense or strongly stretched brushes because then $\phi > 1$ is predicted and/or $h > 1$. Also, in both cases, the (end-)density profile remains invariant with grafting density and values for v and w. In reality, at high density, leading to strong stretching, the density profiles change, deviating more and more from a parabolic profile, with end-density profiles becoming more and more peaked.

To describe these effects in an off-lattice model we introduce two novel elements. First of all, we extend the Gaussian stretching model, eq 2, to account for finite-stretching for continuum (off-lattice) chains. Second, we use an off-lattice expression for volume interactions between polymer chains, envisioned to be made up of spherical beads.

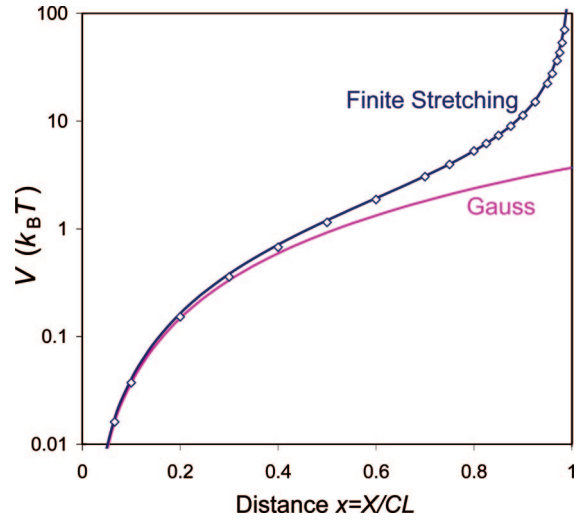

Figure 1. Stretching potential as a function of the distance relative to the chain contour length (CL). Comparison of empirical eq 10 (blue line), with exact solution of the continuum model from ref 11 (diamonds) evaluated up to x^{1000}. Gaussian limit given by eq 2 can be used up to $x \sim 0.4$.

Strong stretching in a continuum model was analyzed in refs 11 and 20. Unfortunately, no simple analytical result is available for the SCF potential V for a strongly stretched continuum chain. However, fortunately, it is possible to derive the Taylor expansion of V. It turns out that only even powers in x are required (x^2, x^4, etc.). The correct prefactors V_k for the x^{2k} terms ($k = 1, 2,...$) are given in Table 1 of ref 11, which start at the Gaussian value of $V_1 = 3/8 \cdot \pi^2$ and go down gradually to level off at a value slightly above 2. In this table the first 30 prefactors are given (required up to x^{60}). For the present paper we analyzed the expansion up to x^{1000} and found that the prefactors very closely approach 2 (the prefactor V_{500} for x^{1000} is calculated as 2.002). This more complete expansion is important to consider for stretching degrees $x > 0.9$. Since the exact expansion[11] is not very convenient for analysis, a more simple empirical expression

$$V(x) = 2\frac{x^2}{k} \frac{2 - \frac{4}{5}x^2}{1 - x^2} \tag{10}$$

will be considered here.

We used the expansion of ref 11 as a benchmark to verify the SCF potential of eq 10. In Figure 1 results of eq 10 (blue line) are compared with the results of the expansion given in Table 1 of ref 11 (diamonds), expanded up to x^{1000}. The factor $2x^2/(1 - x^2)$ correctly takes into account the limit $V_k \rightarrow 2$.[11] It must be noted that the empirical eq 10 does *not* have the first term correct. Instead, expanding eq 10 in terms of x^2 gives for $k = 1$ a prefactor of 4, which theoretically is required to be $3/8 \cdot \pi^2 \sim 3.70$. However, this error hardly matters for realistic modeling because the actual error made, either absolutely (in k_BT) or relatively, is very small. Indeed, across all possible values of the height and the potential V (4 orders of magnitude considered), Figure 1 shows that eq 10 represents a very accurate description of the exact continuum model and agrees very well with the Gaussian model at low values of the distance x.

To describe polymer volumetric interactions, we take an approach that is based on the Carnahan−Starling (CS) equation-of-state from liquid-state theory for hard-sphere mixtures. To apply these theories to polymers, we need to replace in the description

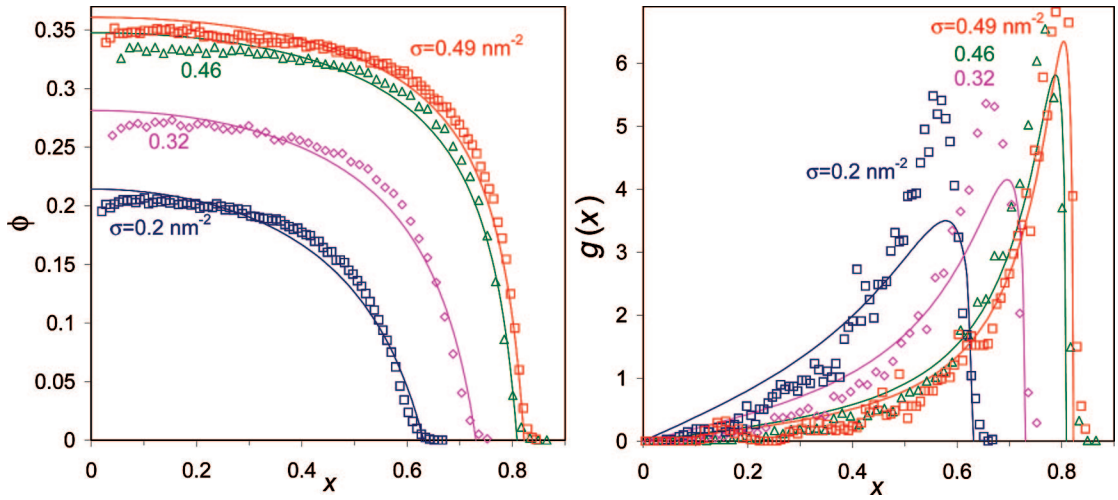

Figure 2. Profiles of the total polymer density, $\phi(x)$, and end density, $g(x)$, vs distance scaled to contour length, x, as a function of grafting density, σ ($k = d = 1$ nm) for the neutral brush model based on the strong-stretching limit of the SCF equation including corrections for finite stretching and high polymer density. Values for $g(x)$ are scaled with the grafting density, $\sigma^{4/3}$. Symbols are MD results from He et al.[14]

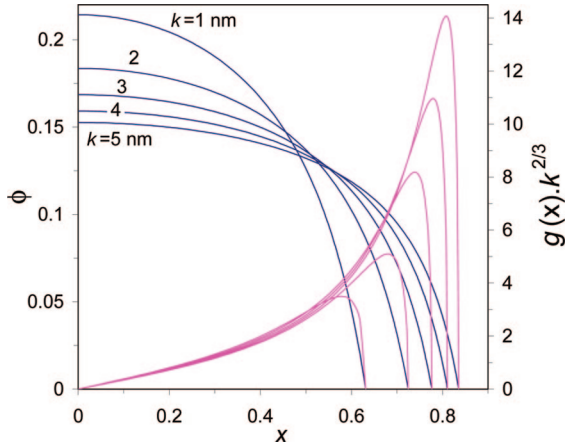

Figure 3. Profiles of the total polymer density, $\phi(x)$ (blue, left axis), and end density, $g(x)$ (pink, right axis), as a function of Kuhn length k for neutral brushes ($d = 1$ nm, $\sigma = 0.2$ nm^{-2}). The end distribution is scaled with $k^{2/3}$.

the polymer chain as a string of spherical beads.[23–25] These spheres do not necessarily need to be "touching", but this will be assumed from this point onward. Thus, per chain of contour length CL we have a number of CL/d beads, where d is the bead diameter. The assumed bead diameter does not have to be equal to the monomer length but can be used as a measure of the specific volume of the polymer chain. When the theory is used to describe simulations with hard-sphere polymers[14] we should ideally set d equal to the size of the spheres in the simulation. The bead diameter is also not necessarily equal to the Kuhn length k, which can be independently varied. Now, to apply the liquid-state theory for polymers, we must make one modification, namely, to leave out the polymer segment concentration from the entropic factor, ξ_0. [For short chains, we can make a modification and count each chain once in ξ_0, but this will not be done here.] This is analogous to the approach in Flory−Huggins (lattice) theory where (for sufficiently high N) also the entropic contribution to the interaction between chains becomes zero.

This approach results in the following expression for $\mu(\phi)$ due to volumetric effects

$$\mu(\phi)\cdot d = \phi\frac{7-7\phi+2\phi^2}{(1-\phi)^3} + \ln(1-\phi) = \sum_{\lambda=1\ldots\infty}(\lambda^2+4\lambda+2-\lambda^{-1})\phi^\lambda = 6\phi+\frac{27}{2}\phi^2+\ldots \quad (11)$$

where the diameter d is implemented to define μ as the potential

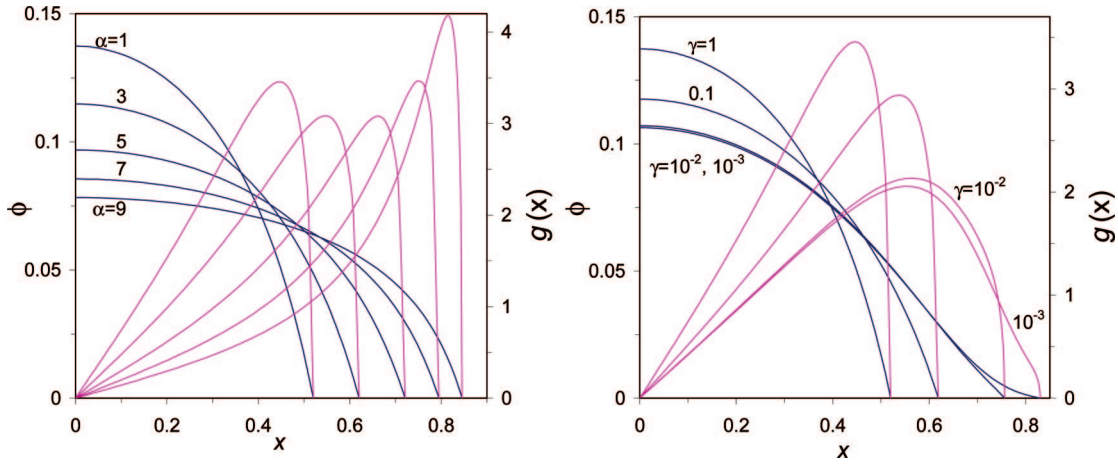

Figure 4. Profiles of the total polymer density, $\phi(x)$ (blue, left axis), and end-density, $g(x)$ (pink, right axis), for polyelectrolyte brushes ($d = 1$ nm, $k = 1$ nm, $\sigma = 0.1$ nm^{-2}). (a) As function of charge α for fixed ionic strength ($\gamma = 1/\alpha$). (b) As function of ionic strength via charge parameter γ ($\alpha = 1$ nm^{-1}).

per unit chain length, required for it to be applicable in eq 1. Note that this somewhat awkward expression is simply a direct, explicit, relation for $\mu(\phi)$ as a function of local concentration ϕ, which can thus be expanded in ϕ, giving a more familiar expression, with the first virial coefficients given by $v = 6$ and $w = 13.5$. Note that a similar expression is applied to polymers in ref 23 (eq 15), but there the polymer segments were erroneously not excluded from ξ_0. Consequently, the resulting expression is the standard Carnahan−Starling result for the contribution of excluded volume to the potential of "free" spheres in a monodisperse mixture. To obtain eq 11 as given above, an additional term $-\phi/(1-\phi) + \ln(1-\phi)$ needs to be added to eq 15 of ref 23.

To eq 11 we can add an enthalpic term, such as $-2\chi\phi$, which we will not consider, and an electrostatic contribution, μ^{elec}, which we will analyze next. When the polymer is charged and has volume, first of all an osmotic, or ion pressure, term must be added, given by[23]

$$\mu^{\text{ion pressure}}(\phi)\cdot d = 2n_\infty v_{\text{bead}}(\cosh y - 1) \tag{12}$$

where n_∞ is the ionic strength of the background salt solution with dimension one over volume, v_{bead} the bead volume, given by $v_{\text{bead}} = \pi/6\cdot d^3$, and y the local dimensionless electrostatic potential (multiply y by the thermal voltage k_BT/e to obtain the dimensional voltage). Equation 12 is based on ions of zero volume, which are unable to penetrate the volume, ϕ, that is occupied by polymer. If the ions are assumed to permeate all space, eq 12 must be left out of the theory. In this paper we will only consider monovalent ions of zero volume, though the extended CS approach makes it straightforward to implement nonzero ion volume and other absorbing spherical species (see refs 23 and 24).

Next, the electrostatic contribution to μ is given by[23]

$$\mu^{\text{elec}} = z\alpha y \tag{13}$$

for polymer with a fixed charge α (per unit length), where z is the charge sign of the chain (we only consider pure polycations or polyanions here) and α defined as a positive number. Note that y will vary over the brush coordinate, as will be explained below. For ionizable polymers we can describe α by[23]

$$\alpha = \frac{\alpha_0}{1 + 10^{z(\text{pH}-\text{p}K)}e^{zy}} \tag{14}$$

where pH is the background pH and pK the intrinsic pK value, a thermodynamic number not influenced by ionic strength or pH. Equation 14 only considers the (de)protonation equilibrium of the chains and excludes adsorption of other ions, while it considers purely acidic or basic chains for with only a single proton can be attached/released per ionizable group (i.e., multivalent and/or zwitterionic sites are not considered). The magnitude of the maximum charge per unit length is given by α_0. In the case of ionizable (annealed) brushes, μ^{elec} is given by[23]

$$\mu^{\text{elec}} = \alpha_0 \ln\left(1 - \frac{\alpha}{\alpha_0}\right) \tag{15}$$

To obtain the electrostatic potential, y, local electroneutrality will be assumed at each position. Note that instead of assuming local electroneutrality, it is also possible to use the full Poisson−Boltzmann equation in the brush model,[23] but in that case analysis of the end-density profiles is no longer possible, at least not in the manner as will be explained below. Local electroneutrality requires

$$2n_\infty(1-\phi)\sinh y = z\alpha d\frac{\phi}{v_{\text{bead}}} \tag{16}$$

where the term $1 - \phi$ exactly follows from the extended CS models if the ions are volumeless. The term can be left out if the ions are assumed to be able to permeate all the space in the brush. In that case, eq 12 must be omitted as well.

In this Note we only consider polymer with fixed charge. In that case we can combine eqs 12, 13, and 16 to obtain

$$\mu(\phi)\cdot\alpha^{-1} = \sqrt{\left(\frac{\phi}{1-\phi}\right)^2 + \gamma^2} - \gamma + \text{asinh}\left\{\gamma^{-1}\frac{\phi}{1-\phi}\right\} \tag{17}$$

where the parameter γ is given by

$$\gamma = \frac{2n_\infty v_{\text{bead}}}{\alpha d} \tag{18}$$

At very low ionic strength or high charge, $\gamma \ll 1$ and eq 17 simplifies to

$$\mu(\phi)\cdot\alpha^{-1} = \frac{\phi}{1-\phi} + \ln\left\{\frac{2}{\gamma}\frac{\phi}{1-\phi}\right\} \tag{19}$$

The dimensionless charge parameter γ increases linearly with ionic strength and is inversely proportional to chain charge density α. For zero charge α, or a very high ionic strength n_∞, the parameter γ goes to infinity, $\gamma = \infty$, and the potential μ of eq 17 is zero, and as expected the neutral brush results.

To calculate the polymer density profile, $\phi(x)$, the above equations suffice. In particular, the expression for V from eq 10 is inserted in eq 1 as well as expressions for $\mu(\phi)$ as given in the most general case by the summation of eqs 11 and 17. Subsequently, eq 1 is solved at each position in the brush under the constraint of overall mass conservation as given by eq 3.

Next we can calculate the end-density profile $g(x)$ which is a bit more convoluted. We use the method as given in ref 11 (namely eq 13 there) which (slightly modified) gives $g(x)$ as

$$g(x) = \frac{1}{\sigma\varepsilon}\frac{\text{d}V(x)}{\text{d}x}\int_0^{x^*}\frac{\text{d}\phi}{\text{d}\nu}\,\text{d}x' \tag{20}$$

where ε is the volume per unit chain length as explained above. The second term, $\text{d}V(x)/\text{d}x$, simply follows from differentiation of eq 10 and is given by

$$\frac{\text{d}V(x)}{\text{d}x} = \frac{8}{5}\frac{x}{k}\frac{2x^4 - 4x^2 + 5}{(1-x^2)^2} \tag{21}$$

The upper integration limit, x^*, follows for each value of x implicitly from the equality

$$V(x^*) = V(h) - V(x) \tag{22}$$

with the required expressions for V from eq 10. The argument within the integration term, $\text{d}\phi/\text{d}\nu$, is the most complicated to solve. The integration parameter ν equals $\nu = V(h) - V(x) - V(x')$, and when executing the differentiation $\text{d}\phi/\text{d}\nu$, both $V(h)$ and $V(x)$ are constant. The procedure is to use ν as the left-hand side of eq 1, insert the required expressions for $\mu(\phi)$ on the right-hand side, and execute the differentiation $\text{d}\phi/\text{d}\nu$. This is only possible analytically for very simple relations between μ and ϕ, and therefore we will make use of the evident formula $\text{d}\phi/\text{d}\nu = 1/(\text{d}\nu/\text{d}\phi)$.

Based on eq 11 for neutral brushes $\text{d}\nu/\text{d}\phi$ is given by

$$\frac{\text{d}\nu}{\text{d}\phi} = \frac{1}{d}\frac{6 + 3\phi - 4\phi^2 + \phi^3}{(1-\phi)^4} \tag{23}$$

which we insert in eq 20 (note that numerator and denominator need to be flipped around). At each x' we numerically find the required ϕ from the implicit expression $\nu = \mu$, which we give for completeness, and is given for neutral brushes by

$$\frac{2}{k}\cdot\left(h^2\frac{2-\frac{4}{5}h^2}{1-h^2}-x^2\frac{2-\frac{4}{5}x^2}{1-x^2}-x'^2\frac{2-\frac{4}{5}x'^2}{1-x'^2}\right)=\frac{1}{d}\cdot\left\{\phi\frac{7-7\phi+2\phi^2}{(1-\phi)^3}+\ln(1-\phi)\right\} \quad (24)$$

For charged brushes, the additional contribution to $d\nu/d\phi$ follows from eq 17 and is given by

$$\frac{d\nu}{d\phi}=\alpha\cdot(1-\phi)^{-3}\cdot\left(\left(\frac{\phi}{1-\phi}\right)^2+\gamma^2\right)^{-1/2} \quad (25)$$

which for low γ (low ionic strength or high charge) simplifies to $d\nu/d\phi = \alpha\cdot(1-\phi)^{-2}\cdot\phi^{-1}$. The additional term required in eq 24 equals α times the right-hand side of eq 17.

Results and Discussion

Results for neutral brushes are given in Figure 2 and are based on a Kuhn length of $k = 1$ nm and a bead size of $d = 1$ nm. Also shown are results of molecular dynamics simulations by He et al.[14] which are based on a bead size of unity (dimensionless units) and an average distance between adjacent beads of $a = 0.97$ using $N = 64$ or $N = 128$ beads in the simulation. These simulations are similar to those of ref 10 but done for higher grafting density (in ref 10 the highest grafting density is 0.20 nm^{-2} assuming a sphere size of 1 nm). To correct for the difference in the simulations between a and d (required to make our calculations applicable to the MD results), we divided the distance coordinate in their work by a.

The MD simulations show the typical features (not contained in our theory) of a depletion layer near the grafting surface and an extended tail in the density profile. Despite these differences, the agreement between theory and MD simulation is remarkably good, taking into account that the theory does not contain any fitting parameters. First of all, the values for the brush heights that are obtained agree very well. Second, the increasing deviation from a parabolic profile with higher grafting density as obtained in the simulations is very well reproduced in the theory, though the MD data show a slightly more pronounced "block" profile (defined by a flat profile in the bulk of the brush and a steep decrease in ϕ near the edge). This is also the reason why the prediction for the end distribution $g(x)$ is not perfect either. Certainly at the lower grafting densities of σ equal to 0.20 and 0.32 nm^{-2}, the theoretical profile is much less peaked than the $g(x)$ profile obtained from the MD simulations. Interestingly, at the higher grafting densities of $\sigma = 0.46$ and 0.49 nm^{-2}, the agreement in $g(x)$ profiles becomes rather exact (note that for $\sigma = 0.49$ nm^{-2} one MD data point at $g(x) = 3.16$ is not shown in Figure 2b).

In Figure 3 we show results of the continuum theory for the influence of Kuhn length on the predicted (end-)density profiles. This is interesting to consider because in the lattice-based SCF models the Kuhn length cannot be varied independently of particle (lattice) size. This is possible in the present continuum model. Results are as predicted, with for higher Kuhn length more extended profiles with a more peaked end-density distribution.

Now that the continuum theory has been applied successfully to describe neutral brushes, it is possible to extent its application range to polyelectrolyte brushes. To that end we analyze for the relatively low grafting density of $\sigma = 0.10$ nm^{-2} the effect of the charge α and charge parameter γ on brush profiles in Figure 4. Note that for a given α a change in γ corresponds to a change in ionic strength. Thus, from this point we will treat γ as a measure of the ionic strength. As expected, with increasing charge α the density profiles expand and become more similar to a block profile. Now, a decrease in γ might be expected to give a similar result. However, with decreasing ionic strength the brush expansion is much less pronounced, and we do not go toward the block profile. Instead, a long tail in the density profile develops with decreasing γ. This difference was also reported clearly in ref 17 where they used a Gaussian stretching potential and a lattice-based expression for volumetric interactions, and assumed that the point ions could permeate the full brush volume. End-point distribution was not yet reported there. Here we report this end-point distribution as well and show that with increasing charge α the position of the maximum in the end-point distribution shifts toward the edge of the brush (from 14% from the edge at $\alpha = 1$ to 4% at $\alpha = 9$), while with decreasing ionic strength, γ, the position of the maximum in the end-point distribution shifts away from the edge (14% at $\gamma = 1$ to 34% away from the edge at $\gamma = 10^{-3}$), while the end-point distribution also develops a very nonmonotonic profile.

A comparison of the theoretical results with MD simulations for charged brushes[26,27] shows that the almost flat density profiles in the bulk of the brush obtained in MD simulations are not completely reproduced by our theory.

Conclusions

We presented a semianalytical theory for neutral and charged monodisperse brushes under the strong-stretching limit of the self-consistent-field equation including corrections for finite stretching and nondilute conditions. We already find peaked end-density distributions at experimentally accessible grafting densities such as 0.2 nm^{-2}. For neutral brushes we obtain almost quantitative agreement with molecular dynamics simulations by He et al.[14] at sufficiently high grafting densities. For charged brushes we show that increasing charge and decreasing ionic strength have very different effects on the end-density distribution, the maximum of which moves toward the edge of the brush with increasing charge but moves away from the edge when the ionic strength is decreased.

Acknowledgment. We kindly thank Dr. Gui-Li He (Xiamen University, China) and Dr. Holger Merlitz (Leibniz Institut für Polymerforschung, Germany) for providing the MD simulation data and for very useful comments during preparation of this manuscript.

References and Notes

(1) Currie, E. P. K.; Wagenmaker, M.; Cohen.Stuart, M. A.; van Well, A. A. *Physica B* **2000**, *283*, 17.
(2) Tsujii, Y.; Ohno, K.; Yamamoto, S.; Goto, A.; Fukuda, T. *Adv. Polym. Sci.* **2006**, *197*, 1.
(3) Milner, S. T. *Science* **1991**, *251*, 905.
(4) Birshtein, T. M.; Amoskov, V. M. *Polym. Sci., Ser. C* **2000**, *42*, 172.
(5) Coluzza, I.; Hansen, J. P. *Phys. Rev. Lett.* **2008**, *100*, 016104.
(6) Skvortsov, A. M.; Pavlushkov, I. V.; Gorbunov, A. A.; Zhulina, E. B.; Borisov, O. V.; Pryamitsyn, V. A. *Polym. Sci. USSR* **1988**, *30*, 1706.
(7) Milner, S. T.; Witten, T. A.; Cates, M. E. *Macromolecules* **1988**, *21*, 2610.
(8) Zhulina, E. B.; Pryamitsyn, V. A.; Borisov, O. V. *Polym. Sci. USSR* **1989**, *31*, 205.
(9) Shim, D. F. K.; Cates, M. E. *J. Phys. (Paris)* **1989**, *50*, 3535.
(10) Murat, M.; Grest, G. S. *Macromolecules* **1989**, *22*, 4054.
(11) Amoskov, V. M.; Pryamitsyn, V. A. *J. Chem. Soc., Faraday Trans.* **1994**, *90*, 889.
(12) Amoskov, V. M.; Pryamitsyn, V. A. *Macromol. Theory Simul.* **2003**, *12*, 223.
(13) Amoskov, V. M.; Birshtein, T. M. *Polym. Sci., Ser. B* **2003**, *45*, 1384.
(14) He, G. L.; Merlitz, H.; Sommer, J. U.; Wu, C.-X. *Macromolecules* **2007**, *40*, 6721.
(15) Wijmans, C. M.; Scheutjens, J. M. H. M.; Zhulina, E. B. *Macromolecules* **1992**, *25*, 2657.
(16) Israëls, R.; Leermakers, F. A. M.; Fleer, G. J.; Zhulina, E. B. *Macromolecules* **1994**, *27*, 3249.
(17) Misra, S.; Varanasi, S.; Varanasi, P. P. *Macromolecules* **1989**, *22*, 4173.

(18) Borisov, O. V.; Leermakers, F. A. M.; Fleer, G. J.; Zhulina, E. B. *J. Chem. Phys.* **2001**, *114*, 7700.
(19) Scheutjens, J. M. H. M.; Fleer, G. J. *J. Phys. Chem.* **1979**, *83*, 1619.
(20) Amoskov, V. M.; Pryamitsyn, V. A. *Polym. Sci., Ser. A* **1995**, *37*, 731.
(21) Pryamitsyn, V. A.; Leermakers, F. A. M.; Fleer, G. J.; Zhulina, E. B. *Macromolecules* **1996**, *29*, 8260.
(22) Amoskov, V. M.; Birshtein, T. M.; Mercurieva, A. A. *Macromol. Theory Simul.* **2006**, *15*, 46.
(23) Biesheuvel, P. M.; Leermakers, F. A. M.; Cohen Stuart, M. A. *Phys. Rev. E* **2006**, *73*, 011802.
(24) de Vos, W. M.; Biesheuvel, P. M.; de Keizer, A.; Kleijn, M. J.; Cohen Stuart, M. A. *Langmuir* **2008**, *24*, 6575.
(25) Zhou, F.; Biesheuvel, P. M.; Choi, E.-Y.; Shu, W.; Poetes, R.; Steiner, U.; Huck, W. T. S. *Nano Lett.* **2008**, *8*, 725.
(26) Seidel, C. *Macromolecules* **2003**, *36*, 2536.
(27) Kumar, N. A.; Seidel, C. *Macromolecules* **2005**, *38*, 9341.

MA800828C